Indonesian Journal of Electrical Engineering and Computer Science
Vol. 9, No. 3, March 2018, pp. 764~770
ISSN: 2502-4752, DOI: 10.11591/ijeecs.v9.i3.pp764-770

An Non Destructive Test for the Detection of Weld Defects Using Image Processing

V. Kalaiselvi, D. John Aravindhar
Research Scholar, CSE Department, Hindustan University, Kelambakam, Chennai, Tamil Nadu 603103, India

Article Info

Article history:

Received Sep 9, 2017
Revised Dec 20, 2017
Accepted Jan 7, 2018

Keywords:

CAD
EM algorithm
Image Segmentation
Gaussian Filter X-ray
Weld defects

ABSTRACT

Welding is a fabrication of joining materials into one component. Defects are unavoidable during the welding process, and hence the inspection of welds is a most important task in many industries. In this work, a Computer Aided Detection (CAD) system is designed to detect weld defects based on image processing techniques. It is a non-destructive testing which uses X-ray images. The proposed system mainly consists of three stages; gradient image formation, filtration by Gaussian pyramidal filters algorithm and segmentation by Expectation and Maximization (EM) algorithm. In this study, GD X-ray weld image database is used to evaluate the proposed system. The performance analysis of the proposed system is done by measuring the sensitivity, specificity, and accuracy of the segmented image with the help of its corresponding ground truth images.

Corresponding Author:

V. Kalaiselvi
Research Scholar, CSE Department,
Hindustan University,
Kelambakam, Chennai, Tamil Nadu 603103, India
Email: vkalaiselvi@rediffmail.com

1. INTRODUCTION

The detection of welding defects is a major concern in any industrial productivity unit. Generally, the welding quality depends upon the voltage, current, welding duration and most importantly the electrodes quality that are used for welding. X-ray radiography is the widely used to detect weld defects. Some of the weld defect detection and segmentation methods are discussed in this section.

1.1 Background

The segmentation of reflected laser lines in robotic arc welding is described in [1]. The 2D intensity distribution is modeled to detect the reflected laser line. It consists of three effective methods; spline enhancement, gradient detection filter, and threshold approach. Some of the major defects like small chips burr or dirt that causes the defects in the welded spots are discussed in [2]. For the detection of these defects, algorithms like Hough circle detection and colour segmentation methods are used. Also, by combining the algorithms like morphological and circle detection algorithms in the vision system, the faults can be identified.

An automatic weld defect segmentation system based on a multi-step radiographic image enhancement algorithm is discussed in [3]. At first, enhancement is performed by linear weighting between the contrast limited adaptive histogram equalization image and the original radiographic images. Then the anisotropic diffusion filtering is used for smoothing, and as a final step, the fuzzy enhancement algorithm is used for filtering the images. An automatic system for the extraction of defects from the radiographic weld images is discussed in [4]. At first, the weld images are pre-processed to increase the quality of the image,

and then Fuzzy C Means (FCM) segmentation algorithm is used to detect weld defects from which the 3D contour plots are plotted by using the extracted features.

A modified background subtraction method for real-time weld defect detection algorithm is discussed in [5]. It is based on the assumption that the pixel intensities of the background in an image sequence are fixed. The weld defects are detected based on the distribution of background pixels that follows a Gaussian distribution with maximum probability. The segmentation approaches are compared and evaluated in [6] for weld defect images. The identified defects are compared with ideal segmentation map in terms of miss-segmented pixels like compactness, location, and connectivity.

A method for the identification of the location of the laser strip on a weld seam tracking is explained in [7]. It is done by applying the Radon transform and also preserves the information of the laser stripe. Then the inverse Radon transform is applied so that the noises are removed. At last, the groove areas are segmented by the improved fast FCM clustering algorithm. An improved Otsu 2D image segmentation algorithm for the requirement of the underwater welding V-seam tracking is discussed in [8]. The algorithm makes a discriminate change in a domain partition of the 2D histogram by adding a relevant variable. Additionally, an optimal thresholding is obtained by enlarging the search step of the thresholding.

A method of segmenting the second category of defects in the welding joints is discussed in [9]. It makes use of the digitized radiographic image in case of low or noisy contrast images. The combination of the contrast enhancements, histogram equalization, and image thresholding processes are used for the segmentation of defects. A segmentation method for the identification of defects in the X-ray weld images is discussed in [10]. As the X-ray weld images are of low-contrast and noisy in nature, the digitized radiographic weld images are used for the segmentation. It is mainly based on a thresholding method known as multiple thresholding along with the support vector machine algorithm.

A segmentation method used to detect the defects on the welded surface is discussed in [11]. The defects are smaller in size and shape and also have low contrast level characteristics which are caused due to the non-uniform illuminations. It uses level set active contour algorithm in which the centre-surround feature saliency map is used to reduce the clustering background. A machine vision welding robot for LED filament welding is designed in [12]. It uses image segmentation algorithm like grey level transformation, edge detection, and two value transformation for processing the segmentation procedures.

A method of color image segmentation using joint color texture histogram based on region merging algorithm is discussed in [13]. It uses both the information of texture histogram and the color histogram for measuring the similarities of various regions and to guide the process region margining. The sagittal image segmentation to get aorta in a gray level image is discussed in [14]. It is a semi automatic segmentation process to segment the sagittal MRI image base that is connected to the labeling method components. A method based on watermarking technique for obtaining the image originality is discussed in [15]. The identification of objects and the small area of chicken eggs are done by using the bounding box and the centroid.

1.2 Problem Statement

a. The major harmfulness and the weakness of welding defects in the steeled structure are as follows:
b. The segmentation of the weld image whose intensity and in-homogeneities of the same object can be disturbed.
c. The problem of boundary leakage at weak edges is a major drawback that they rely much on the gradient value.
d. Though the arrangements of uniform illumination are made very correctly, there is a vibration of illumination occurred during the welding process.

1.3 The Proposed Solution

To overcome these problems an efficient CAD system for weld defect detection based on various image processing techniques on X-ray weld images is presented. The proposed system consist three main steps like formation of gradient images, filtration by Gaussian pyramidal filters algorithm and Expectation and Maximization (EM) algorithm for final segmentation.

The paper organization is as follows: Section 2 gives the methods and materials used for the proposed CAD system for weld defects detection. The next section gives the results of the weld defect detection system and section 4 concludes the CAD system.

2. RESEARCH AND METHOD

The proposed system for weld defect detection is considered as an image segmentation problem. Figure 1 shows the flow of the CAD system for weld defects.

2.1. Gradient Image Formation

In the first stage, the intensity variation (Δ) in both horizontal (x) and vertical direction (y) is computed. For a 2D dimensional original image denoted by I, the intensity variation in x and y direction are given below:

$$\Delta x = I(x+n, y) - I(x-n, y) \tag{1}$$

$$\Delta y = I(x, y+n) - I(x, y-n) \tag{2}$$

where n is the smallest integer. From the intensity variations, gradient magnitude image is created which shows the edges present in the original image I. The gradient magnitude image G is computed as

$$G(x, y) = \sqrt{\Delta x^2 + \Delta y^2} \tag{3}$$

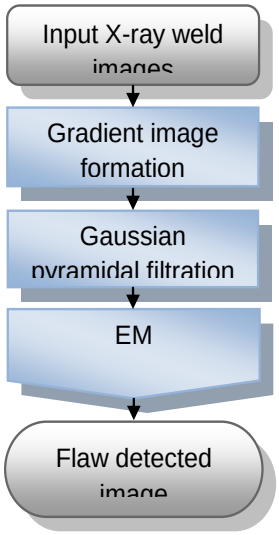

Figure 1. CAD system for weld defects

The above equation is used to obtain the gradient magnitude image. Figure 2 (a) shows the X-ray weld image and Figure 2 (b) shows the gradient magnitude image obtained using (3).

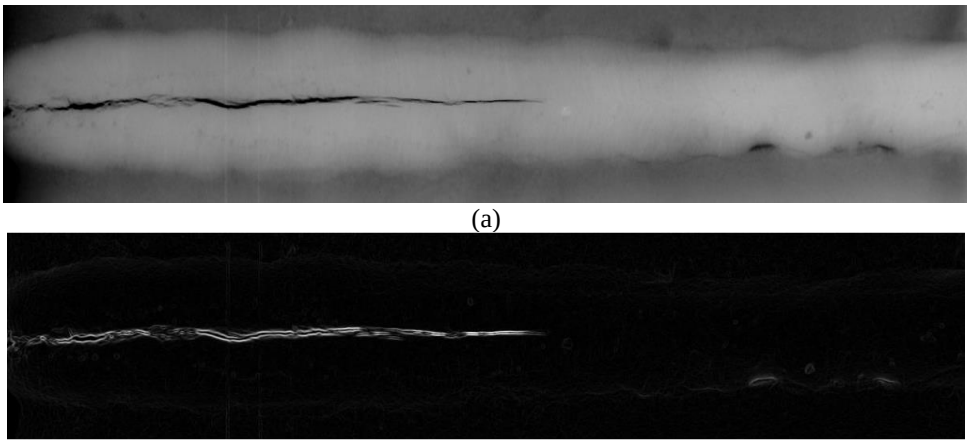

(a)

(b)

Figure 2. (a) X-ray weld image (b) Gradient magnitude image

2.2. Gaussian Pyramidal Filtration

In order to fine tune the edges obtained from the gradient magnitude image, Gaussian pyramidal filter algorithm is employed in the second stage. The concept of the Gaussian pyramid represents a multi-resolution scene where each frame that makes up an image flow is progressively filtered and sub-sampled to easily deal with the search of objects at different scales. The Gaussian pyramidal filter process for G(x, y) is as follows:

$$GPF_0(x,y) = G(x,y) \text{ forlevel,l} = 0 \tag{4}$$

$$GPF_1(x,y) = \sum_{m=-2}^{2} \sum_{n=-2}^{2} w(m,n) GPF_{l-1}(2x+m, 2y+n) \tag{5}$$

where $w(m,n)$ is a weighted function for all identical levels that are termed as generating the kernel properties at level l+1. Figure 3 shows the application of Gaussian pyramidal filtration on Gradient magnitude image in Figure 2 (b).

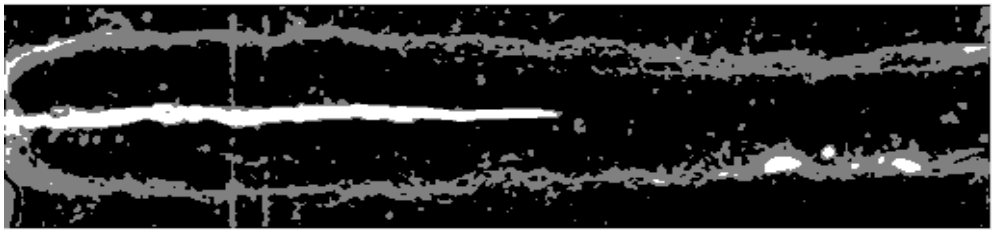

Figure 3. Gaussian pyramidal filtered image

2.3. EM Segmentation

In this stage, weld defects are detected or segmented by using EM segmentation algorithm with the help of the filtered image. The procedure for EM algorithm closely follows the K-means clustering algorithm. The accuracy of EM algorithm depends on the initial cluster values. Let us assume that these values are very close to the ground truth data. As the name implies the first step begins with an Expectation step (E) for pixel z as in Eqn. 6.

$$E[z_{ij}] = -\frac{p(x = x_i \mid \mu = \mu_i)}{\sum_{n=1}^{k} p(x = x_i \mid \mu = \mu_n)} \tag{6}$$

Using the above Eqn. 6, the weight for pixel z concerning partition j is computed. For each image, this step computes weights for every pixel. After E step, the maximization step (M) begins.

$$\mu_j \leftarrow \frac{1}{m} \sum_{i=1}^{m} E[z_{ij}] x_i \tag{7}$$

Using the above Eqn. 7, the weight of j partition is updated. Then the E step is repeated using the new set of partition until there is no change in the partition values. By using this algorithm, the flaws that are present in the weld image are detected. Figure 4 shows the final segmented output image obtained by EM approach for the image shown in Figure 3.

Figure 4. Weld defect detection by EM segmentation

3. RESULT AND DISCUSSION

In this study, GD X-ray weld image database [16] is used to evaluate the proposed system. The performance of the system is analyzed regarding sensitivity, specificity, and segmentation accuracy using the ground truth images. These measures are widely used in many image processing applciations [17-19].The output image obtained by the proposed algorithm and the ground truth images that are used for the performance analysis are shown in Figure 5. The CAD system for weld defects is implemented in MATLAB R2015b.

The qualitative analysis from Figure 5 clearly shows that the proposed CAD system segments the weld defects from the original X-ray welded images in an efficient manner. In order to quantitatively analyze the CAD system, the following measures; sensitivity, specificity and accuracy are used. These measures can be easily obtained from the confusion matrix. It is made from the defect regions (white pixels) and non-defect regions (black pixels).

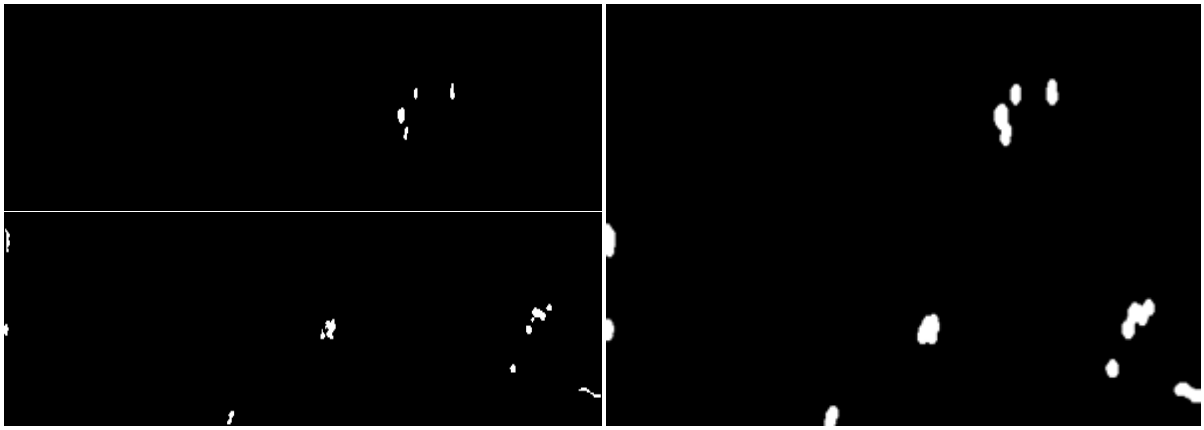

(a) **(b)**

Figure 5. (a) Ground truth image (b) Weld defect detection by the proposed system

Table 1. Confusion matrix of CAD system for weld defect detection

Test outcome	Actual Class	
	Positive (weld defects)	Negative(non-defect/good)
Positive (weld defects)	True Positive (TP) – Weld defect pixel is correctly identified as defected	False Positive (FP) – Good pixel is incorrectly identified as weld defect
Negative (non-defect/good)	False Negative (FN) - Weld defect pixel is incorrectly identified as good pixel	True Negative (TN) – Good pixel is correctly classified as good pixel

From the confusion matrix, sensitivity, specificity, and accuracy are computed for each image concerning the segmented and the ground truth images. Their definitions are as follows:

a. Sensitivity

It takes only the positive cases (weld defects). It is the ratio between the total TP decisions to the number of actual positive cases. It is defined by eqn. 8.

$$Sensitivity = \frac{TP}{(TP + FN)} \quad (8)$$

b. Specificity

It deals with only the negative cases (non-defect regions). It is the ratio between the total TN decisions to the number of actual negative cases. It is defined by Eqn. 9.

$$\text{Specificity} = \frac{\text{TN}}{(\text{FP} + \text{TN})} \quad (9)$$

c. Accuracy

It deals with both positive cases (weld defects) and negative cases (no defect regions). It is defined by Eqn. 10.

$$Accuracy = \frac{\text{TP} + \text{TN}}{(\text{TP} + \text{FN} + \text{FP} + \text{TN})} \quad (10)$$

Table 2 shows the computed performance measures of the system on GD X-ray image database. All the images in GD X-ray image database are used for the evaluation.

Table 2. Performance of the system on GD X-ray image database database

S. No.	Accuracy (%)	Sensitivity (%)	Specificity (%)
1	89.66	89.89	86.67
2	97.94	97.93	99.75
3	99.73	99.74	94.74
4	99.48	99.51	88.17
5	99.44	99.44	100
6	98.82	98.83	95.98
7	95.42	95.72	87.73
8	99.48	99.48	100
9	90.10	89.61	98.03
10	98.62	98.61	100
Avg	96.87	96.88	95.11

From Table 2, it is observed that the CAD system detects 96.88% of weld defects and 95.11% of non-defect regions. Also, it provides an average accuracy of 96.87% on GD X-ray image database. The measures sensitivity and specificity show how correctly the segmented output images are matched with its ground truth images. The comparison of the proposed system is made with the other successful weld image segementation method. It is focused on the database used and the output parameters like sensitivity, specificity and the accuracy of the segmentation system. Table 3 shows the comparative analysis. It is clear that the proposed system provides better results than others in terms of accuray and sensitivity.

Table 3. Comparision of proposed weld image segmentation with other methods

Database	Technique used	Sensitivity	Specificity	Accuracy
GD X-rays	PCA based SVM model [20]	87.28	96.31	90.75
GD X-rays	Off-Center Saliency Map Computation with Level Set Active Contour Energy Formulation [21]	-	-	87 %
GD X-rays	Radiographic patterns based geometric features and Neural network classifier [22]	83.9	74.8	80.6
GD X-rays	Proposed method	96.88	95.11	96.88

4. CONCLUSION

In this paper, a non-destructive test method for the detection of the welding defects is proposed using X-ray images. The weld defects reduce the quality of the materials. As they are not visible to the naked eye, it requires a CAD system to identify the weld defects. The identification of weld defects is done by using the three stages; gradient image formation, filtration by Gaussian pyramidal filter algorithm, and

segmentation by EM segmentation algorithm. Results show that the CAD system provides 96.88% (sensitivity), 95.11% (specificity), and an average accuracy of 96.87% on GD X-ray image database.

REFERENCES

[1] Wang Z. *Automatic Segmentation of Fuzzy Laser Lines with Sub-Pixel Accuracy from the Uneven Background during Robotic Arc Welding*. IEEE 7th International Conference on Intelligent Systems, Modeling and Simulation. 2016; 157-162.

[2] Kim C, Han DS, Kim JK, Kim BI. *Automatic detection of defective welding electrode tips using colour segmentation and Hough circle detection*. IEEE Region 10th Conference. 2016; 1371-1374.

[3] Dang C, Gao J, Wang Z, Chen F, Xiao Y. *Multi-step radiographic image enhancement conforming to weld defect segmentation*. IET Image Processing. 2015; 9(11): 943-950.

[4] Sundaram M, Jose JP, Jaffino G. *Welding defects extraction for radiographic images using C-means segmentation method*. IEEE International Conference on Communication and Network Technologies. 2014; 79-83.

[5] Liao Z, Sun J. Image segmentation in weld defect detection based on modified background subtraction. IEEE 6th International Congress on Image and Signal Processing. 2013; 2: 610-615.

[6] Goumeidane AB, Khamadja M. *Merging discrepancy measures for region-based segmentation results evaluation and comparison: Application to thresholded weld defect radiographic images.* IEEE 8th International Symposium on Image and Signal Processing and Analysis. 2013; 78-82.

[7] Liu X. *Image processing in weld seam tracking with laser vision based on radon transform and FCM clustering segmentation*. IEEE International Conference on Intelligent Computation Technology and Automation. 2010; 2: 470-473.

[8] Jia J, Li H, Jia Z. *Image segmentation of the underwater welding V-seam image based on improved two-dimensional Otsu algorithm.* IEEE 6th International Conference on Fuzzy Systems and Knowledge Discovery. 2009; 5: 397-400.

[9] Mahmoudi A, Regragui F. *Welding defect detection by segmentation of radiographic images*. IEEE WRI World Congress on Computer Science and Information Engineering. 2009; 7: 111-115.

[10] Mahmoudi A, Regragui F. *Fast segmentation method for defects detection in radiographic images of welds*. IEEE/ACS International Conference on Computer Systems and Applications. 2009; 857-860.

[11] Gharsallah MB, Braiek EB. *Image segmentation for defect detection based on level set active contour combined with saliency map*. IEEE 16th International Conference on Sciences and Techniques of Automatic Control and Computer Engineering. 2015; 388-392.

[12] Zhang S, Zhang Y, Yang T, Jin C, Shang G. *Research on LED filament spot welding robot based on machine vision*. IEEE International Conference on Information and Automation. 2016; 1510-1514.

[13] Zhang J, Xie C, Song L, Li R, Chen H. Robust Image Segmentation Using LBP Embedded Region Merging. *TELKOMNIKA (Telecommunication Computing Electronics and Control)*. 2016; 14(1): 368-377.

[14] Riminarsih D, Karyati CM, Mutiara AB, Wahyudi B, Ernastuti E. MRI Sagittal Image Segmentation from Patients with Abdominal Aortic Aneurysms. *TELKOMNIKA (Telecommunication Computing Electronics and Control)*. 2016; 14(3): 1105-1112.

[15] Yudhana A, Sunardi S, Saifullah S. Segmentation Comparing Eggs Watermarking Image and Original Image. *Bulletin of Electrical Engineering and Informatics*. 2017; 6(1): 47-53.

[16] GD X-ray image database: http://dmery.ing.puc.cl/index.php/material/gdxray/

[17] Sonawane JM, Gaikwad SD, Prakash G. *Microarray data classification using dual tree m-band wavelet features*. International Journal of Advances in Signal and Image Sciences. 2017; 3(1): 19-24.

[18] Vijaya Arjunan R. ECG Signal Classification Based on Statistical Features with Svm Classification. *International Journal of Advances in Signal and Image Sciences*. 2016; 2(1): 5-10.

[19] Sonia R. Melanoma Image Classification System by NSCT Features and Bayes Classification. *International Journal of Advances in Signal and Image Sciences*. 2016; 2(2): 27-33.

[20] Mu W, Gao J, Jiang H, Wang Z, Chen F, Dang C. *Automatic classification approach to weld defects based on PCA and SVM*. Insight-Non-Destructive Testing and Condition Monitoring. 2013; 55(10): 535-539.

[21] Ben Gharsallah M, Ben Braiek E. Weld inspection based on radiography image segmentation with level set active contour guided off-center saliency map. *Advances in Materials Science and Engineering*. 2015; 1-10.

[22] da Silva RR, Siqueira MH, de Souza MPV, Rebello JM, Caloba LP. Estimated accuracy of classification of defects detected in welded joints by radiographic tests. *NDT & e International*. 2005; 38(5): 335-343.